sustainable chemistry

MDPI

Article

Effect of Pretreatment of Orange Peel with Deep Eutectic Solvents Before Acid Hydrolysis to Produce Reduced Sugars

María del Carmen Carreño-de-León, Nicolas Flores-Alamo *, Fredy Cuellar-Robles, Juan José Luna-Torres and Daniela Gutiérrez-López *

División de Estudios de Posgrado e Investigación, Instituto Tecnológico de Toluca, Tecnológico Nacional de México, Av. Tecnológico s/n, Col. Agrícola Bellavista, Metepec 52149, Mexico; mcarrenod@toluca.tecnm.mx (M.d.C.C.-d.-L.); fcuellarr@toluca.tecnm.mx (F.C.-R.); jlunat@toluca.tecnm.mx (J.J.L.-T.)

* Correspondence: nfloresa@toluca.tecnm.mx (N.F.-A.); daniela.gl@toluca.tecnm.mx (D.G.-L.)

Abstract

Currently, approximately 80% of the energy used worldwide comes from fossil fuels. The production of bioethanol from agro-industrial waste requires pretreatment due to the latter's rigid structure and resistance to degradation. In this work orange peel (OP) was pretreated with deep eutectic solvents (DESs), varying the molar ratio of the mixture to delignify the OP, exposing cellulose and hemicellulose, in order to improve the yield in the acid hydrolysis process with H_3PO_4 to produce reduced sugars. SEM, FTIR, and XRD were used to evaluate the structural changes in OP with and without pretreatment. Optimal pretreatment was achieved using ChCl/U at a 1:4 molar ratio, yielding 31.58 g of reducing sugars per 100 g of pretreated OP after 150 min, compared with 12.09 g of reducing sugars per 100 g of untreated OP after 300 min. The holocellulose content after pretreatment increased by 28%. Significant differences were found in the reducing-sugar yield and the structure of OP with and without pretreatment; DESs are useful for biomass delignification, thus enabling increased reducing-sugar production through acid hydrolysis.

Keywords: orange peel; deep eutectic solvents; reducing sugar

1. Introduction

Energy demand is linked to population growth. This problem has caused significant concern and could be addressed using biofuels from lignocellulosic waste [1], due to the high content of readily fermentable sugars present in the cellulose and hemicellulose allowing the production of biofuels from biomass. The biomass could be from agriculture, industrial parks, or municipal solid waste [2,3]. Biomass includes lignocellulose, consisting mainly of cellulose (23–50%), lignin (13–31%), and hemicellulose (12–29%) [4].

The process to obtain biofuels can be summarized as three steps: pretreatment, saccharification, and fermentation. Biomass pretreatment is responsible for releasing the polymer chains of cellulose and hemicellulose for subsequent saccharification [5]. During the pretreatment process, the biomass undergoes various reactions (degradation and depolymerization) that lead to the breaking of intermolecular and intramolecular bonds between cellulose, hemicellulose, and lignin. This leads to improved accessibility of the carbohydrates during saccharification (hydrolysis), improving the yield of the final product [6,7]. This process is classified into four types: physical, chemical, physicochemical, and biological. The effectiveness of the pretreatment is determined by the complex structure of

Check for updates

Academic Editor: Raffaele Cucciniello

Received: 19 September 2026
Revised: 9 October 2026
Accepted: 12 October 2026
Published: 14 October 2026

Copyright: © 2026 by the authors. Licensee MDPI, Basel, Switzerland. This article is an open access article distributed under the terms and conditions of the Creative Commons Attribution (CC BY) license.

biomass, energy consumption, economic viability, and environmental impact [8]. Therefore, an effective pretreatment is necessary to overcome the physical and chemical barriers to biomass hydrolysis.

Chemical pretreatments with acids, bases, and ionic liquids have been used; however, their application may come with problems such as corrosion, a high cost, and environmental impacts like air and water pollution. Another drawback of these chemical pretreatments is the formation of inhibitors that hinder the metabolic activity of microorganisms in the fermentation process, negatively impacting the efficiency of biomass bioconversion [9]. Therefore, it is important to find a suitable pretreatment that is environmentally, socially, and economically advantageous.

The use of deep eutectic solvents (DESs) is gaining significant attention worldwide as they are considered environmentally friendly solvents with many advantages over other conventional methods [10]. However, further research is needed to combine DESs with other chemical or physical methods to achieve an optimal process. DESs are typically formed by combining a hydrogen-bond acceptor (HBA) and a hydrogen-bond donor (HBD) at specific molar ratios that promote eutectic behavior and extensive hydrogen bond interactions [11].

Deep eutectic solvents (DESs) increase the deconstruction of lignocellulosic biomass by disrupting the interactions between cellulose, hemicellulose, and lignin. Their strong hydrogen-bonding capacity reduces biomass crystallinity and increases accessibility of the structural components. In acidic DES systems, protons catalyze the β-O-4 bonds in lignin, depolymerizing it. In a deep eutectic solvent (DES), the components are typically classified as hydrogen-bond acceptors (HBAs) and hydrogen-bond donors (HBDs); HBAs contain atoms with lone electron pairs and can accept hydrogen bonds, for example, choline chloride, betaine, tetraethylammonium chloride, tetramethylammonium chloride, and phosphonium salts, while HBDs include urea, glycerol, propylene, glycol, xylitol, and sorbitol [2,10,12,13].

Recent research has aimed to optimize biomass fractionation using DES-like mixtures by coupling them with auxiliary technologies, including microwave irradiation, ultrasonic processing, and the use of enzymes and microorganisms. Furthermore, considerable attention has been devoted to understanding the delignification mechanisms of DES-like systems and developing efficient methods for their recovery and recycling [13].

The aim of this study was to determine the effect of chemical pretreatment with DESs on delignification of orange peel biomass (OP), using choline chloride (ChCl) as an HBA and oxalic acid (OA) and urea (U) as HBDs, with 1:2 and 1:4 molar ratios. After pretreatment, acid hydrolysis kinetics measurements were performed using a 1 M H_3PO_4 solution at 80 and 115 °C. Additionally, the material was characterized before and after pretreatment by using FTIR, SEM, and XRD; the lignin, cellulose, and hemicellulose contents were determined.

2. Materials and Methods

2.1. Chemicals

All the reagents used were analytical grade; choline chloride, acetylacetone, furfural, and dioxane were supplied by Sigma-Aldrich (St. Louis, MO, USA). Acetone, toluene, urea, oxalic acid, phosphoric acid, ethanol, ethyl ether, hydrochloric acid, methanol, and acetic acid were supplied by Jalmek (Monterrey, Mexico); sodium chlorite was supplied by Golden Bell (Jalisco, México); and sulphuric acid was supplied by Silverquim (México, México). All solutions were prepared using distilled water.

2.2. Residue Samples of OP

The OP was obtained from waste produced by juice shops. Excess pulp was removed from the raw material to prevent decomposition, and then the material was cut into pieces and washed with tape water to remove impurities. Thereafter, the OP was dried at 50 °C in a recirculating oven for 72 h; it was then ground and sieved to a particle size less than 250 µm. Finally, it was stored until use. Free extractives (soluble organic compounds such as resins, waxes, and fats) were obtained for the determination of the composition of untreated biomass [14], 8 g of OP powder was treated in a Soxhlet apparatus (Pyrex, New York, NY, USA) with 100 mL of a 1:2 ethanol–toluene mixture; the mixture was boiled until no color change was observed in the siphon of the extractor.

2.3. Chemical Composition

The chemical composition of the OP was determined before and after pretreatment with DESs. The content of cellulose was determined by using the Seifert method [15]. A mass of 2 g of extractive-free or pretreated material was placed in a 50 mL round-bottom flask, and 6 mL of acetylacetone, 2 mL of 1,4-dioxane, and 1 mL of hydrochloric acid were added. The mixture was refluxed for 30 min; the solid was then vacuum-filtered and washed separately with 10 mL of each of the following solvents: methanol, dioxane, and ethyl ether, followed by 5 mL of distilled water. Finally, the sample was dried in a recirculating oven at 105 °C until a constant weight. The final weight corresponded to the cellulose [16].

For holocellulose (the polysaccharide fraction of lignocellulosic biomass composed of cellulose and hemicellulose after lignin removal) measurements, 4 g of extractive-free or pretreated material was placed in a 250 mL two-necked round-bottom flask, and 160 mL of water was added. The mixture was refluxed at 80 °C, heated once, and then 10 drops of acetic acid and 1 g of sodium chlorite were added. After 1 h of constant stirring, the two reagents were added again, and reflux was allowed for four hours more. At the end of the reaction, the mixture was allowed to cool and vacuum-filtered, then washed with cold water and acetone [17]. The filter paper was placed in an oven at 105 °C until a constant weight was reached; the difference between the initial and final weight corresponded to the holocellulose. The hemicellulose was calculated by the difference between the holocellulose and cellulose content.

2.4. Characterization

2.4.1. Fourier Transform Infrared (FTIR) Spectroscopy

An FTIR analysis was performed to determine the main functional groups and the changes in these groups after pretreatment. The sample was dried at 45 °C until constant weight in a recirculating oven and ground using a mortar for subsequent analysis in a Varian 640 FTIR spectrometer at a wavelength range of 4000 to 400 cm^{-1} and a resolution of 4 cm^{-1} for 32 scans.

2.4.2. X-Ray Diffraction (XRD)

X-Ray diffraction was performed to examine the crystallinity of cellulose. It was carried out on a Discovery D8 diffractometer operated at a potential of 35 kV and using kα radiation of 1.5418 Å from a copper electrode. The step size was set to 0.03° with a 2θ diffraction range from 5° to 80°. The crystallinity index (CrI) was calculated using the peak-height method based on the diffraction intensity of the crystalline and amorphous regions using Equation (1) [10]:

$$CrI\ (\%) = \frac{I_2 - I_1}{I_2} \times 100 \quad (1)$$

where I_2 and I_1 are the diffraction intensities of the crystalline region (2θ between 22 and 24°) and the amorphous region (2θ between 16 and 19°), respectively.

2.4.3. Scanning Electron Microscopy (SEM)

SEM was used to monitor morphological changes before and after pretreatment with the DES. The sample was dried at 45 °C for 12 h in a recirculating oven and pulverized in a mortar, then analyzed on a JEOL JSM-590-LD microscope (JEOL Ltd., Akishima, Japan) at 10 kV under low vacuum up to 1000× magnification.

2.5. OP Pretreatment with DES

OP was treated with a DES in two molar ratios to find out the highest percentage of delignification, two different solvents were tested, using choline chloride (ChCl) as the HBA and urea (U) and oxalic acid (OA) as the HBDs, each in HBA:HBD molar ratios of 1:2 and 1:4; these molar ratios were selected to ensure adequate handling of the obtained DESs, as equimolar ratios lead to increased mixture viscosity, making the solvents more difficult to handle and process. The solid fractions were placed in a beaker and stirred at 500 rpm and 60 °C until a homogeneous, clear solution was formed. OP was added, the solvent/solid ratio was 10/1 (g/g), and stirred for 2 h at 80 °C. After the pretreatment time, an antisolvent (water, ethanol, 50:50) was added, and stirring was maintained for 30 min. The solid samples were separated by filtration and dried at 80 °C.

2.6. Acid Hydrolysis Kinetics

Acid hydrolysis was performed with 0.5 M H_3PO_4 [18] at 80 and 115 °C. Each kinetic test was carried out for 5 h, taking samples every 30 min. Each sample was prepared by mixing 0.5 g of pretreated OP with 7 mL of acid solution in screw-cap test tubes to prevent sample evaporation. The tubes were then placed in a HACH 200 digital reactor at the desired temperature. The tubes were allowed to cool at room temperature, the phases were separated by filtration, and the reducing-sugar content of the liquid phase (hydrolysate) was determined by the DNS method and the furfural content by UV–vis spectroscopy at a wavelength of 277 nm. The solid phase was characterized by FTIR, SEM, and XRD.

Acid hydrolysis of OP without pretreatment was performed under the same conditions to determine the efficiency of the pretreatment in order to improve the yield of reducing sugars. The kinetic data were fitted to the Saeman kinetic model [19]; according to their proposal, cellulose hydrolysis proceeds through the breakdown of the glucan polymer into glucose monomers (glucose and xylose principally), followed by the conversion of glucose into secondary decomposition products (furfural); the process involves a series of irreversible and first-order reactions related to the production of monomeric sugars (k_1) and their transformation into inhibitory aldehydes (k_2). This allows the determination of the concentration of monosaccharides as a function of reaction time, according to Equation (2):

$$M = \left[\frac{k_1 P_0}{k_2 - k_1}\right]\left(e^{-tk_1} - e^{tk_2}\right) \quad (2)$$

where M is the concentration of reducing sugars (g of sugar/100 g of raw material), P_0 is the initial concentration of holocellulose (g of holocellulose/100 g of raw material), t is the contact time (min), k_1 is the kinetic constant for the formation of sugars (min^{-1}), and k_2 is the kinetic constant for the degradation of sugars (min^{-1}).

According to Saeman [19] and Ranganathan [20], the kinetic constants obtained from the Saeman model can be used to calculate the relationship between both (k_r), which shows the effect of temperature and acid concentration and represents the balance between sugar formation and sugar degradation. Higher k_r values indicate that the production of

reducing sugars predominates over their degradation, whereas lower values suggest that degradation reactions become more significant than sugar generation. Subsequently, this relationship can be used to determine the optimum reaction time for sugar production (Equation (3)).

$$t_{op} = \frac{1}{k_2(k_r - 1)} In(k_r) \quad (3)$$

The sugar production data were fitted to the described kinetic model using a nonlinear regression in the Origin 8.6 software, which employs the Levenberg–Marquardt method, and the quality of the model fit was evaluated by the R^2 value.

3. Results and Discussion

3.1. Chemical Composition

Table 1 shows the composition of the OP before DES chemical pretreatment. The chemical composition of OP is primarily cellulose, followed by hemicellulose and lignin. Cellulose is the simplest natural polymer to convert into monomers in the fermentation process [21]. The extractive content was similar to that reported by Ortiz [22] (26.73%) and may have consisted of the essential oil content, terpenes, waxes, pigments, and other solvent-soluble compounds commonly found in orange peel. The holocellulose results were like those reported by Ayala [17] (69.09%); however, the lignin content was lower (19.8%). These variations may be attributed to the type of orange and even the growing conditions [23].

Table 1. Chemical composition of OP before pretreatment.

Parameter	Percentage (%)
Extractives	26.24 ± 0.02
Cellulose	41.02 ± 0.23
Hemicellulose	22.35 ± 0.24
Lignin	10.34 ± 0.08

3.2. Fourier Transform Infrared Spectroscopy (FTIR)

The FTIR spectra of untreated orange peel (OP) and DES-pretreated samples exhibited the characteristic absorption bands of lignocellulosic biomass (Figure 1).

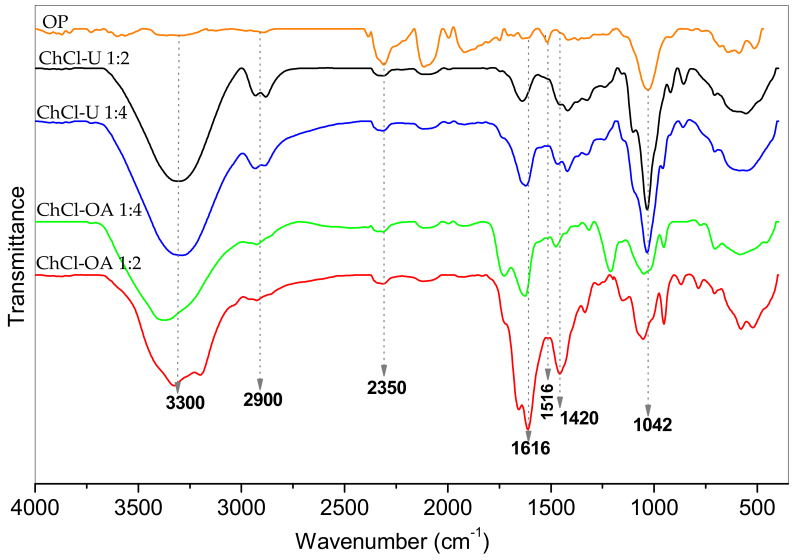


Figure 1. FTIR spectra of orange peel (OP) before and after deep eutectic solvent (DES) pretreatment, showing changes in the characteristic bands of cellulose, hemicellulose, and lignin.

The spectrum of OP showed characteristic bands of lignocellulosic raw material. The characteristic hemicellulose bands were observed at 2900 and 2350 cm^{-1}, attributed to the $-CH_3$, $-CH_2$, and C=O bonds in ketone groups, respectively. The vibration observed at 1042 cm^{-1} corresponds to stretching vibrations of the $-CH_2OH$ and CO groups of cellulose. Finally, lignin exhibited characteristic aromatic ring bands at 1516 and 1616 cm^{-1}, attributed to aromatic skeletal vibrations of the C=C guaiacyl bonds of lignin. The band intensity at 1516 cm^{-1} in untreated OP decreased after pretreatment, which could be attributed to partial depolymerization of lignin [24].

The decrease in the bands around 2350 cm^{-1} can be attributed to the partial removal of hemicellulose after pretreatment. Furthermore, the band at 1042 cm^{-1} was more pronounced in the OP pretreated with ChCl-U than ChCl-OA, also it was shifted to 1055 cm^{-1}. In both cases, cellulose remained in the sample after pretreatment [8,9].

The most notable differences are observed in the intensity of the bands around 3300 cm^{-1} (O-H stretching), 1616–1516 cm^{-1} (aromatic skeletal vibrations associated with lignin), and 1042 cm^{-1} (C-O stretching of polysaccharides). These changes indicate that the different DES molar ratios promoted different extents of lignin removal and modification of the lignocellulosic structure. In particular, the ChCl-OA 1:2 system exhibited stronger changes in the lignin-related region than ChCl-OA 1:4, suggesting a more pronounced fractionation effect. Similarly, differences between ChCl-U 1:2 and ChCl-U 1:4 indicate that the DES composition influenced the accessibility of biomass components and the efficiency of the pretreatment. The peak at 1616 cm^{-1} increased in intensity after the pretreatment, possibly due to the increase in hemicellulose in the sample and maybe traces of residual DES; in addition, a shift to 1640 cm^{-1} in the case of ChCl-U 1:2, and the formation of an additional peak at 1730 cm^{-1} for ChCl-AO 1:4 and at 1630 cm^{-1} for ChCl-AO 1:2, indicate the presence of acetyl groups in the hemicelluloses and the C=O aromatic vibrational stretching of the lignin, respectively [8,24,25].

The broad band observed at approximately 3300 cm^{-1} was attributed to O-H stretching vibrations associated with cellulose, hemicellulose, lignin, and pectin. The lower intensity of the broad absorption band centered at approximately 3300 cm^{-1} in untreated orange peel could be related to the drying process carried out prior to analysis. Drying to constant weight may have reduced the moisture content of the biomass, thereby decreasing the contribution of O-H stretching vibrations associated with adsorbed water [25]. Nevertheless, changes in hydrogen-bonding interactions among structural carbohydrates and lignin may also have contributed to the observed spectral behavior. The increased intensity and broadening of this band after DES pretreatment suggest alterations in the hydrogen-bonding network and increased exposure of hydroxyl groups [9,24].

The absorption band around 2900 cm^{-1}, assigned to the C-H stretching vibrations of aliphatic groups, remained relatively unchanged after pretreatment, suggesting that the carbohydrate backbone was largely preserved [26]. This band was more pronounced in samples pretreated with ChCl-U at both molar ratios, whereas it was nearly absent in samples treated with ChCl-OA [27]. In addition, the appearance of a new band was observed at approximately 1420 cm^{-1}, characteristic of the formation of crystalline cellulose; it was more intense in ChCl-OA [28]. The changes are possibly due to the severity of the acidic pretreatment with oxalic acid.

The differences indicate that structural modifications occurred in OP after pretreatment due to exposing the cellulose and hemicellulose, but there were no significant differences when increasing the HBD ratio.

3.3. X-Ray Diffraction (XRD) Analysis

The samples before (Figure 2) and after (Figure 3) DES pretreatment were analyzed by X-ray diffraction to find out the impact of the pretreatment on the crystalline structure of OP cellulose.

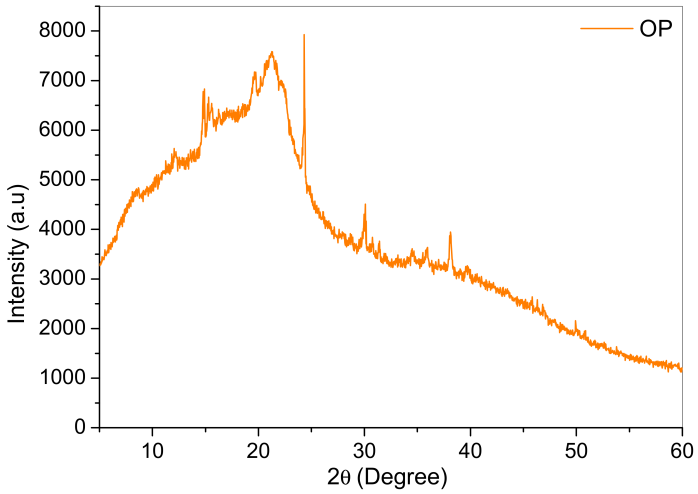


Figure 2. XRD diffractogram of untreated OP used as a reference material, showing the characteristic diffraction peaks of the native lignocellulosic structure before DES pretreatment.

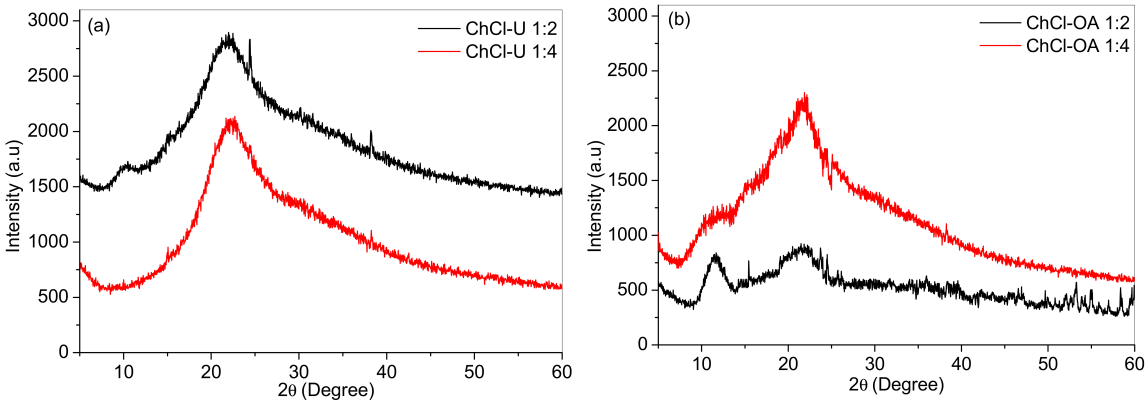


Figure 3. XRD diffractograms of OP pretreated with DESs, (**a**) ChCl-U and (**b**) ChCl-OA, highlighting changes in the diffraction pattern and cellulose crystallinity resulting from the pretreatment.

The diffractograms show significant structural changes in OP after pretreatment. Before pretreatment, it exhibited low-intensity 2θ diffraction peaks near 16° and 22°, corresponding to amorphous and crystalline type I cellulose; defined peaks (24°, 30°, and 39°) attributed to the inorganic phase of OP were also observed. Pushparani and Baskar [29] attribute these peaks to calcium oxalate, a crystal naturally produced by citrus plants. The crystallinity index (CrI) of untreated OP was 17%, characteristic of a lignocellulosic material, due to the high content of amorphous components: pectin, hemicellulose, and lignin [30].

After pretreatment, the peak at 22° increases sharply with ChCl-U (Figure 3), preserving the type I cellulose; in contrast, the peak at 16° weakens, which can be attributed to the loss of amorphous components of the OP, such as lignin, hemicellulose, and extractives [8,31]. The XRD spectra of the orange peel samples were modified after ChCl-OA pretreatment. In particular, the ChCl-OA 1:4 sample showed a more prominent diffraction feature in the region around 2θ = 21–22° compared with the broader diffraction profile of untreated orange peel and the ChCl-OA 1:2 sample. This behavior may indicate an increased relative contribution of ordered cellulose domains after pretreatment, potentially

associated with the removal of amorphous components from the lignocellulosic matrix [11]. Nevertheless, the XRD patterns alone cannot conclusively demonstrate an increase in cellulose crystallinity. Furthermore, the possible presence of residual traces of DES components in the recovered solid cannot be completely excluded (Figure S1).

3.4. Scanning Electron Microscopy (SEM/EDS)

Micrographs of untreated and pretreated OP at 500 (right) and 1000 times magnification (left) are shown in Figure 4. The untreated OP (Figure 4a) exhibited a uniform and smooth surface, indicating a rigid and highly ordered surface structure. The compact structure of the untreated OP was disrupted after pretreatment with a DES. Following pretreatment with ChCl-U (Figure 4b,c), the surface roughness increased, revealing prominent cracks that exposed the internal structures and fibers [8,10]. This result indicated that the pretreatment removed some of the external fibers by disrupting the lignocellulosic network and provided an accessible surface to facilitate subsequent hydrolysis [32]. The OP structure pretreated with ChCl-OA (Figure 4d,e) shows agglomerations without evident cracks, this is probably due to the partial removal of lignin and the increase in crystalline cellulose observed by the FTIR and XRD analyses.

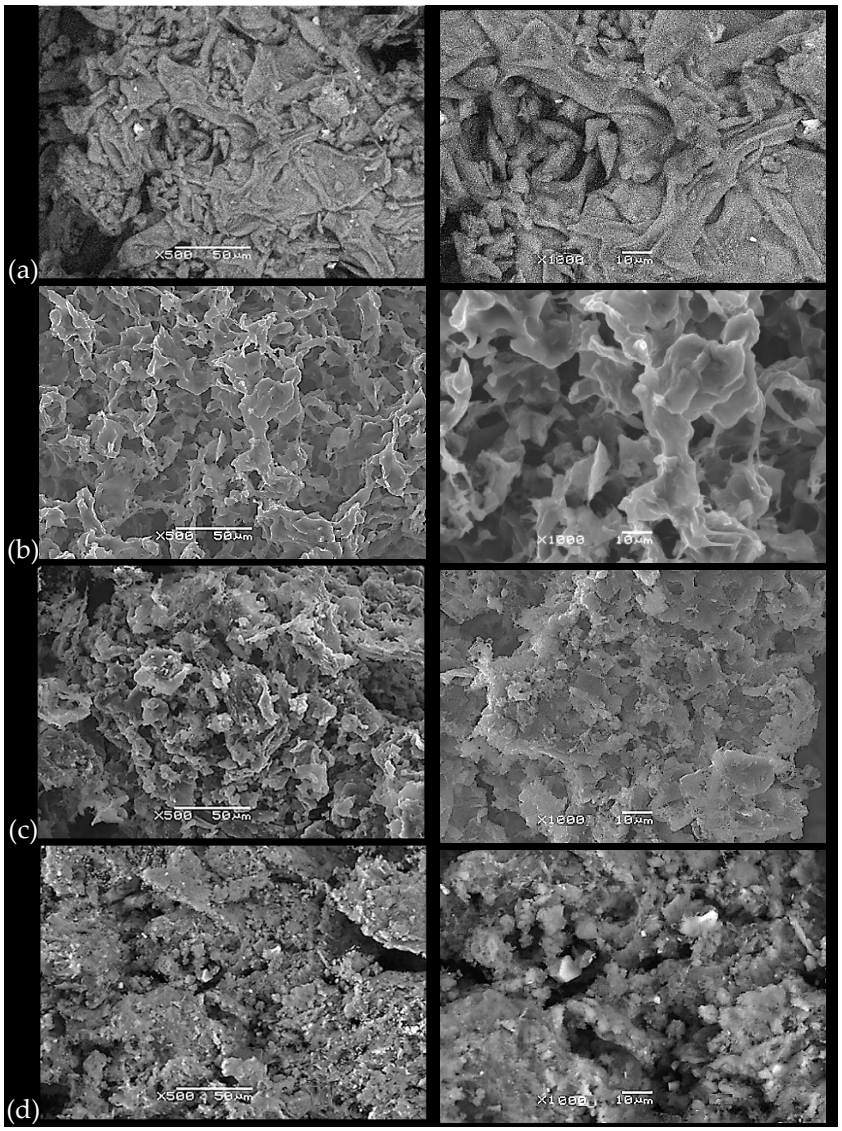


Figure 4. *Cont.*

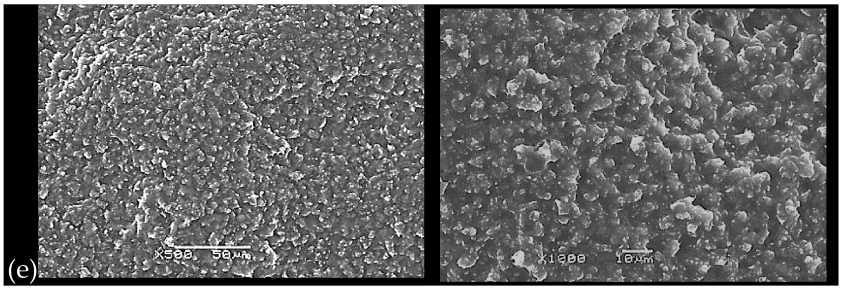


Figure 4. Micrographs of OP (**a**) untreated and pretreated with (**b**) ChCl-U 1:2, (**c**) ChCl-U 1:4, (**d**) ChCl-OA 1:2, and (**e**) ChCl-OA 1:4 at 500 (**right**) and 1000 times magnification (**left**).

Table 2 presents the atomic percentage of each element of OP with and without pretreatment.

Table 2. EDS analysis of OP with and without pretreatment.

Element	OP	ChCl-U		ChCl-OA	
		1:2	**1:4**	**1:2**	**1:4**
C	58.60	60.09	65.75	69.2	75.24
O	40.45	27.43	26.75	24.26	18.31
K	0.39	-	-	-	-
Ca	0.56	0.53	0.54	-	-
Cl	-	11.95	6.96	6.54	6.45

The C and O contents change after pretreatment because of the holocellulose transformation. The presence of K was observed in untreated OP; Cl was observed after pretreatment with DES, attributed to the interaction of the chloride ion from ChCl with the carbohydrate chains. Finally, Ca was observed in the micrographs of untreated and ChCl-U pretreated OP, confirming the presence of calcium oxalate crystals (XRD). Conversely, Ca was not observed in the ChCl-OA pretreatment, possibly because the acidic nature of OA dissolved these crystals.

3.5. Influence of DES Pretreatment on Chemical Composition of OP

The pretreatment of lignocellulosic biomass with deep eutectic solvents mainly involves the disruption of the lignin–carbohydrate complex through hydrogen-bond interactions and acid-catalyzed cleavage of ether linkages. This promotes lignin solubilization, partial hemicellulose hydrolysis, and increased cellulose accessibility. As a result, the recalcitrant structure of biomass is substantially broken down, facilitating subsequent conversion of cellulose and hemicellulose into fermentable sugars [33].

Following contact of the OP with the DES at each of the ratios, the percentages of lignin, hemicellulose, and cellulose remaining in the solid fraction were determined. The chemical composition of OP (Table 3) showed the highest delignification with ChCl-U (1:2). Using the untreated OP composition as the reference, lignin decreased from 10.34% to 7.65%, while holocellulose increased from 63.37% to 81.65%. The lignin reduction was calculated according to Equation (4):

$$\text{Lignin reduction } (\%) = \frac{10.34 - 7.65}{10.34} \times 100 = 26.0\% \quad (4)$$

which corresponds to a relative decrease in lignin content. Similarly, the increase in holocellulose content was calculated according to Equation (5):

$$\text{Holocellulose increase } (\%) = \frac{81.65 - 63.37}{63.37} \times 100 = 28.8\% \quad (5)$$

corresponding to a relative increase in holocellulose content after pretreatment. Therefore, pretreatment with ChCl-U (1:2) resulted in the highest delignification and holocellulose enrichment, whereas increasing the DES molar ratio did not further improve pretreatment efficiency.

Table 3. Chemical composition of pretreated OP.

DES	Relation of DES	% Lignin	% Holocellulose	% Hemicellulose	% Cellulose
ChCl-U	1:2	7.65 ± 0.15	81.65 ± 0.09	27.98 ± 0.17	53.67 ± 0.28
	1:4	8.56 ± 0.25	72.80 ± 0.11	24.97 ± 0.05	47.89 ± 0.02
ChCl-OA	1:2	9.65 ± 0.20	63.56 ± 0.21	21.67 ± 0.07	41.89 ± 0.18
	1:4	8.34 ± 0.25	61.96 ± 0.05	21.98 ± 0.22	39.98 ± 0.21
OP		10.34 ± 0.05	63.37 ± 0.10	22.35 ± 0.05	41.02 ± 0.19

In contrast, pretreatment with ChCl-OA at a 1:2 molar ratio resulted in a holocellulose content comparable to that of untreated OP, whereas a decrease was observed when the ChCl-OA molar ratio was increased to 1:4. These findings are consistent with the FTIR spectra (Figure 1), which showed no significant structural changes. A similar behavior was reported by Li et al. [34].

Overall, among the DES formulations investigated in this study, the ChCl-U systems, particularly the 1:2 molar ratio, showed the highest effectiveness for lignin removal when compared with the ChCl-OA systems and untreated orange peel. This behavior may be associated with the presence of chloride ions and their interactions with the cellulose and hemicellulose structures. Furthermore, acidic HBDs have been reported to promote lignin removal by facilitating the disruption of lignin–carbohydrate complexes [35].

3.6. Acid Hydrolysis Kinetics

The pretreatment of lignocellulosic biomass with deep eutectic solvents promotes the disruption of lignin–carbohydrate complexes, partial lignin removal, and a reduction in cellulose crystallinity. These structural modifications increase the accessibility of cellulose and hemicellulose to acid attack during the subsequent hydrolysis step. Under acidic conditions, hemicellulose is hydrolyzed to pentose sugars, mainly xylose, whereas cellulose is depolymerized into glucose. At higher reaction severities, these sugars undergo dehydration reactions, leading to the formation of furfural from pentoses and 5-hydroxymethylfurfural from hexoses [33].

Figure 5 shows the kinetics for reducing-sugar production from OP before and after pretreatment, where the scatter and dashed lines represent the experimental data and fits to the Saeman model, respectively, at 80 and 115 °C. An increase in sugar production was observed over time; however, after approximately 150 min, it decreased, possibly due to sugar decomposition [19].

The maximum sugar yield of 31.58 g of sugar/100 g in 150 min at 80 °C was achieved with the pretreated OP (ChCl-U 1:4) and the yield without pretreatment was 12.09 g of sugar/100 g in 300 min. A similar production (29 g of sugar/g of material) was observed at 115 °C and ChCl-U 1:2 in 120 min.

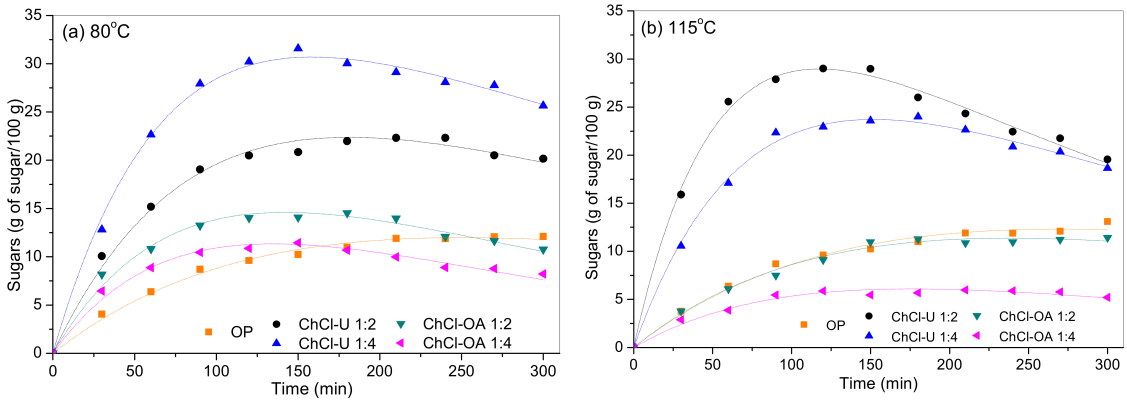


Figure 5. Acid hydrolysis kinetics at two OP temperatures with and without pretreatment fitted to the Saeman model.

Sugar production was similar with the acid hydrolysis of pretreated OP with ChCl-OA 1:2 and without pretreatment at 115 °C and decreased with the 1:4 ratio. Possibly due to the decrease in hemicellulose and cellulose, however, the crystallinity increased. According to Das et al. [5], this behavior was due to the formation of black liquor, which is mainly composed of soluble lignin and hemicellulose, resulting in a lower content of carbohydrates available for conversion into reducing sugars in the solid. Morales-Huerta et al. [36] observed that increasing the molar ratio of HBDs leads to carbohydrate degradation reactions, reducing the sugar yield.

Table 4 presents the fit of the experimental data to the Saeman kinetic model, with R^2 values > 0.98 for each hydrolysis. The calculated optimum reaction time is consistent with the observations in Figure 5, since the maximum sugar production for ChCl-U 1:2 at 115 °C was reached in 120 min, and the optimum time determined with that temperature was 117 min.

Table 4. Kinetic and statistical parameters determined with the Saeman model.

Pretreatment Conditions	Hydrolysis Temperature (°C)	k_1	k_2	R^2	k_r	t_{op}
		$(min^{-1}) \times 10^{-3}$				
OP	80	5.72	2.65	0.992	2.16	251
	115	5.37	2.44	0.986	2.20	269
ChCl-U 1:2	80	9.88	2.68	0.991	3.69	181
	115	17.39	3.35	0.994	5.19	117
ChCl-U 1:4	80	13.31	2.34	0.995	5.69	158
	115	12.14	3.07	0.995	3.95	152
ChCl-OA 1:2	80	10.73	4.32	0.983	2.48	142
	115	5.95	2.84	0.991	2.10	238
ChCl-OA 1:4	80	10.51	5.04	0.982	2.09	134
	115	7.01	4.54	0.966	1.54	176

It can be observed that the pretreatment with ChCl-U considerably favored the production rate (k_1) and the production of sugars achieved, compared with OP without pretreatment. The values of the kinetic constant k_1 for ChCl-U 1:2 increased as a function of temperature and molar ratio; the highest value was 17.39 × 10^{-3} min^{-1} at 115 °C. For ChCl-U 1:4, the value of k_1 decreased slightly as the temperature rose, possibly because of the more severe pretreatment leading to thermal degradation. In the case of ChCl-OA, although the k_1 value increased compared to OP, no increase in the production of reducing sugars was observed. This can probably be attributed to the combined effect of the increased cellulose crystallinity of OP (Figure 3) and the fact that the chemical composition

did not change after pretreatment (Table 3). Similar behavior was observed by Procentese et al. [37] in the enzymatic hydrolysis of corn cob pretreated with DESs.

The k_r factor, given in Table 4, is defined as the numerical relationship between the kinetic constants (k_1/k_2). Values greater than 1 mean that the value of k_2 is less than k_1, which suggests that under these operating conditions, hydrolysis is favorable for the production of reducing sugars.

In addition to the simple sugars obtained from the depolymerization of cellulose and hemicelluloses, hydrolysates can contain desirable chemicals, including furfural, 5-hydroxymethylfurfural (5-HMF), and acetic acid. Furfural is the main product that typically inhibits further fermentation of the hydrolysate, while 5-HMF and acetic acid are produced in smaller quantities [38]. Therefore, furfural formation was also measured in the sugar production. Figure 6 shows furfural production during hydrolysis at the two temperatures, with and without pretreatment.

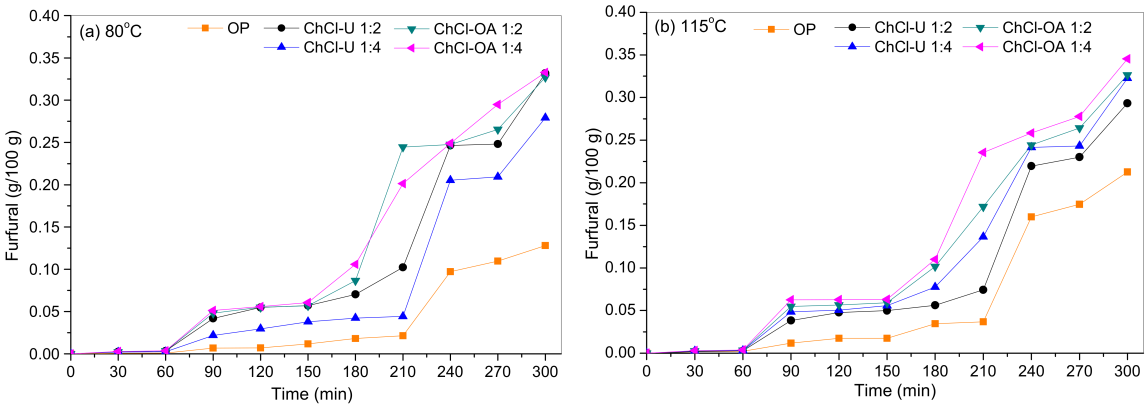


Figure 6. Furfural production profiles obtained from untreated and pretreated OP, showing the impact of pretreatment on sugar degradation and furfural formation.

As observed, the furfural production behaviors at 80 and 115 °C were similar; increases in both temperature and reaction time favored furfural production, with 0.34 g produced per 100 g of OP; this was the maximum production found (ChCl-OA 1:4 at 115 °C after 300 min). Erkan et al. [39] found that the yeast *Saccharomyces cerevisiae* can tolerate a furfural concentration up to 1 g/L in sugar fermentation processes; therefore, pretreatment with DESs can be a satisfactory option; detoxification strategies before the fermentation process with microorganisms are not necessary when the biomass is pre-treated with DESs.

4. Conclusions

Pretreatment with DESs showed high acid hydrolysis efficiency. After pretreatment with ChCl-U 1:2 with a liquid/solid ratio of 10:1, the holocellulose content increased by 28%, and a maximum yield of reducing sugars of 31.58 g/100 g was obtained after 120 min of hydrolysis. The pretreated OP showed a higher hydrolysis yield compared to the untreated OP, increasing the sugar production rate. The structural changes after pretreatment, observed by SEM, FTIR, and XRD, indicate significant effects of the pretreatment. The results of this study demonstrate the effectiveness of pretreatment of OP with ChCl-U and provide a reference for effective biotransformation. In addition, furfural production was found to be lower than the levels expected to cause significant inhibition in the yeast Saccharomyces cerevisiae, thus there is not any additional detoxification strategies necessary. Pretreatment of OP with ChCl-OA in the ratio 1:2 was effective.

Supplementary Materials: The following supporting information can be downloaded at: https://www.mdpi.com/article/10.3390/suschem7040062/s1, Figure S1: FTIR spectra of deep eutectic solvent (DES) formulations, showing the characteristic bands; ChCl-U 1:2, ChCl-U 1:4, ChCl-OA 1:2, ChCl-OA 1:4.

Author Contributions: D.G.-L. and M.d.C.C.-d.-L.: Writing (original draft), methodology, investigation; N.F.-A.: Writing (review and editing), validation, methodology, data curation; F.C.-R. and J.J.L.-T.: Review and editing, supervision. All authors have read and agreed to the published version of the manuscript.

Funding: This research received no external funding.

Institutional Review Board Statement: Not applicable.

Informed Consent Statement: Not applicable.

Data Availability Statement: The original contributions presented in this study are included in the article/Supplementary Material. Further inquiries can be directed to the corresponding authors.

Acknowledgments: D.G.L. thanks SECIHTI for the postdoctoral fellowship awarded.

Conflicts of Interest: The authors declare no conflicts of interest.

Abbreviations

The following abbreviations are used in this manuscript:

OP	Orange peel
DES	Deep eutectic solvent
ChCl	Choline chloride
U	Urea
OA	Oxalic acid
HBA	Hydrogen-bond acceptor
HBD	Hydrogen-bond donor

References

1. Priya; Singh, P.; Verma, Y.; Avtar, R.; Goswami, C.; Sing, T. Biofuels: An alternative to convencional fueland energy source. *Mater. Today Proc.* **2021**, *48*, 1178–1184. [CrossRef]
2. Liu, Y.; Gao, L.; Chen, L.; Zhou, W.; Wang, C.; Ma, L. Exploring carbohydrate extraction from biomass using deep eutectic solvents: Factors and mechanisms. *IScience* **2023**, *26*, 107671. [CrossRef] [PubMed]
3. Chi, T.; Quoc, N. Developing biomass energy from agricultural by-products in the context of trade development. *Energy Strategy Rev.* **2024**, *54*, 101417. [CrossRef]
4. Hasanov, I.; Raud, M.; Kikas, T. The role of ionic liquids in the lignin separation from lignocellulosic biomass. *Energies* **2020**, *13*, 4864. [CrossRef]
5. Das, N.; Jena, P.K.; Padhi, D.; Mohanty, M.K.; Sahoo, G. A comprehensive review of characterization, pre-treatment and its applications on different lignocellulosic biomass for bioethanol production. *Biomass Convers. Biorefinery* **2021**, *13*, 1503–1527. [CrossRef]
6. Kassaye, S.; Pant, K.K.; Jain, S. Hydrolysis of cellulosic bamboo biomass into reducing sugars via a combined alkaline solution and ionic liquid pretreament steps. *Renew. Energy* **2017**, *104*, 177–184. [CrossRef]
7. Behera, S.; Arora, R.; Nandhagopal, N.; Kumar, S. Importance of chemical pretreatment for bioconversion of lignocellulosic biomass. *Renew. Sustain. Energy Rev.* **2014**, *36*, 91–106. [CrossRef]
8. Xie, W.; Ren, Y.; Jiang, F.; Liang, J.; Du, S.K. Pretreatment of quinoa straw with 1-butyl-3-methylimidazolium chloride and physiochemical characterization of biomass. *Renew. Energy* **2020**, *146*, 1364–1371. [CrossRef]
9. Azizan, A.; Jusri, N.A.A.; Azmi, I.S.; Abd Rahman, M.F.; Ibrahim, N.; Jalil, R. Emerging lignocellulosic ionic liquid biomass pretreatment criteria/strategy of optimization and recycling short review with infrared spectroscopy analytical know-how. *Mater. Today Proc.* **2022**, *63*, S359–S367. [CrossRef]
10. Li, C.; Huang, C.; Zhao, Y.; Zheng, C.; Su, H.; Zhang, L.; Huang, L.J. Effect of choline-based deep eutectic solvent pretreatment on the structure of cellulose and lignin in bagasse. *Processes* **2021**, *9*, 384. [CrossRef]
11. Pradhan, D.; Jaiswal, S.; Tiwari, B.K.; Jaiswal, A.K. Choline chloride–oxalic acid dihydrate deep eutectic solvent pretreatment of Barley straw for production of cellulose nanofibers. *Int. J. Biol. Macromol.* **2024**, *281*, 136213. [CrossRef] [PubMed]

12. Li, P.; Yang, C.; Jiang, Z.; Jin, Y.; Wu, W. Lignocellulose pretreatment by deep eutectic solvents and related technologies: A review. *J. Bioresour. Bioprod.* **2023**, *8*, 33–44. [CrossRef]
13. Jančíková, V.; Jablonský, M. Exploiting deep eutectic solvent-like mixtures for fractionation biomass, and the mechanism removal of lignin: A review. *Sustainability* **2024**, *16*, 504. [CrossRef]
14. Sluiter, A.; Ruiz, R.; Scarlata, C.; Sluiter, J.; Templeton, D. *Determination of Extractives in Biomass: Laboratory Analytical Procedure (LAP)*; NREL/TP-510-42619; National Renewable Energy Laboratory (NREL): Golden, CO, USA, 2008; pp. 1–16.
15. Danielewicz, D.; Surma-Ślusarska, B.; Żurek, G.; Martyniak, D.; Kmiotek, M.; Dybka, K. Selected grass plants as biomass fuels and raw materials for papermaking, part II. Pulp and paper properties. *BioResources* **2015**, *10*, 8552–8564. [CrossRef]
16. Chavez, E.G.S.; Roldán, I.U.M.; Cedeno, F.R.P.; Brienzo, M.; Pereira, J.F.; Masarin, F. Pretreatment of sugarcane by-products using triethylammonium hydrogen sulfate: Assessment of the recovery of cellulosic pulp and lignin. *Biomass Bioenergy* **2026**, *211*, 109182. [CrossRef]
17. Ayala, J.R.; Montero, G.; Coronado, M.A.; García, C.; Curiel-Alvarez, M.A.; León, J.A.; Montes, D.G. Characterization of orange peel waste and valorization to obtain reducing sugars. *Molecules* **2021**, *26*, 1348. [CrossRef] [PubMed]
18. Gutiérrez-Lopez, D.; Carreño-de-León, M.D.C.; Solache-Ríos, M.J.; Gomora-Hernandez, J.C.; Ventura-Cruz, S.; Flo-res-Alamo, N. Kinetic and thermodynamic study on acid hydrolysis of corn cob, rose stem, and pineapple crown. *Chem. Eng. Commun.* **2023**, *210*, 1581–1592. [CrossRef]
19. Saeman, J.F. Kinetics of wood saccharification: Hydrolysis of cellulose and decomposition of sugars in dilute acid at high temperature. *Ind. Eng. Chem.* **1945**, *37*, 43–52. [CrossRef]
20. Ranganathan, S.; McDonald, D.G.; Bakhsi, N.N. Kinetic studies of wheat straw hydrolysis using sulphuric acid. *Can. J. Chem. Eng.* **1985**, *63*, 840–844. [CrossRef]
21. Láinez, M.; Ruiz, H.A.; Castro-Luna, A.A.; Martínez-Hernández, S. Release of simple sugars from lignocellulosic biomass of Agave salmiana leaves subject to sequential pretreatment and enzymatic saccharification. *Biomass Bioenergy* **2018**, *118*, 133–140. [CrossRef]
22. Ortiz, M.; Cardona, C.; Solarte, J. Orange peel waste as a source of bioactive compounds and valuable products: Insights based on chemical composition and biorefining. *Biomass* **2024**, *4*, 107–131. [CrossRef]
23. Niño, R.M.V.; Arteaga, Y.A.; Segura, C.F. Obtención, purificación y aprovechamiento de azúcares reductores a partir de materiales lignocelulósicos. *Rev. Boliv. De Quím.* **2024**, *41*, 10–27. [CrossRef]
24. Sharma, S.; Nargotra, P.; Sharma, V.; Bangotra, R.; Kaur, M.; Kapoor, N.; Bajaj, B.K. Nanobiocatalysts for efficacious bioconversion of ionic liquid pretreated sugarcane tops biomass to biofuel. *Bioresour. Technol.* **2021**, *333*, 125191. [CrossRef] [PubMed]
25. Zhuang, J.; Li, M.; Pu, Y.; Ragauskas, A.J.; Yoo, C.G. Observation of potential contaminants in processed biomass using fourier transform infrared spectroscopy. *Appl. Sci.* **2020**, *10*, 4345. [CrossRef]
26. Jančíková, V.; Jablonsky, M.; Majova, V.; Suty, S. Study of the effects of DES-like mixtures on the properties of unbleached softwood kraft pulp. *Results Chem.* **2024**, *9*, 101670. [CrossRef]
27. Shen, X.J.; Wen, J.L.; Mei, Q.Q.; Chen, X.; Sun, D.; Yuan, T.Q.; Sun, R.C. Facile fractionation of lignocelluloses by biomass-derived deep eutectic solvent (DES) pretreatment for cellulose enzymatic hydrolysis and lignin valorization. *Green Chem.* **2019**, *21*, 275–283. [CrossRef]
28. Mafa, M.S.; Malgas, S.; Bhattacharya, A.; Rashamuse, K.; Pletschke, B.I. The effects of alkaline pretreatment on agricultural biomasses (corn cob and sweet sorghum bagasse) and their hydrolysis by a termite-derived enzyme cocktail. *Agronomy* **2020**, *10*, 1211. [CrossRef]
29. Pushparani, V.P.; Baskar, G. Synthesize and characterization of CaOx crystals against various citrus waste peel extracts: An in vitro study. *Prep. Biochem. Biotechnol.* **2023**, *53*, 353–365. [CrossRef] [PubMed]
30. Najjoum, N.; Grimi, N.; Benali, M.; Chadni, M.; Castignolles, P. Extraction and chemical features of wood hemicelluloses: A review. *Int. J. Biol. Macromol.* **2025**, *311*, 143681. [CrossRef] [PubMed]
31. Bouramdane, Y.; Fellak, S.; El Mansouri, F.; Boukir, A. Impact of natural degradation on the aged lignocellulose fibers of Moroccan cedar softwood: Structural elucidation by infrared spectroscopy (ATR-FTIR) and X-ray diffraction (XRD). *Fermentation* **2022**, *8*, 698. [CrossRef]
32. Qiu, Z.; Aita, G.M.; Walker, M.S. Effect of ionic liquid pretreatment on the chemical composition, structure and enzymatic hydrolysis of energy cane bagasse. *Bioresour. Technol.* **2012**, *117*, 251–256. [CrossRef] [PubMed]
33. Huang, K.; Mohan, M.; Su, K.; Gao, C.; Chen, Y.; Xu, X.; Yanping, C.; Jianming, G.; Yong, X.; Xin, Z.; et al. Deep eutectic solvents in lignocellulosic biorefineries: A comprehensive review of mechanistic insights, molecular modeling, and artificial intelligence. *Green Chem.* **2026**, *28*, 12505–12548. [CrossRef]
34. Li, X.; Tang, W.; He, Y.C. Integrated understanding of acidic deep eutectic solvent choline chloride: Oxalic acid pretreatment to enhance the enzymatic hydrolysis of rape straw. *Ind. Crops Prod.* **2023**, *206*, 117691. [CrossRef]

35. Chen, Y.; Tang, Z.; Tang, W.; Ma, C.; He, Y. Exploration of biomass fractionation and lignin removal for enhancing enzymatic digestion of wheat-stalk through deep eutectic solvent Cetyl trimethyl ammonium chloride:Lactic acid treatment. *Int. J. Biol. Macromol.* **2025**, *306*, 141460. [CrossRef] [PubMed]
36. Morales-Huerta, J.C.; Hernandez-Melendez, O.; Hernández-Luna, M.G.; Manero, O.; Barzana, E.; Vivaldo-Lima, E. An experimental and modeling study on the pretreatment and alkaline hydrolysis of blue agave bagasse in twin-screw extruders. *Ind. Eng. Chem. Res.* **2021**, *60*, 12449–12460. [CrossRef]
37. Procentese, A.; Johnson, E.; Orr, V.; Campanile, A.G.; Wood, J.A.; Marzocchella, A.; Rehmann, L. Deep eutectic solvent pretreatment and subsequent saccharification of corncob. *Bioresour. Technol.* **2015**, *192*, 31–36. [CrossRef] [PubMed]
38. Cieciura-Włoch, W.; Binczarski, M.; Tomaszewska, J.; Borowski, S.; Domański, J.; Dziugan, P.; Witońska, I. The use of acidic hydrolysates after furfural production from sugar waste biomass as a fermentation medium in the biotechnological production of hydrogen. *Energies* **2019**, *12*, 3222. [CrossRef]
39. Erkan, S.B.; Yatmaz, E.; Germec, M.; Turhan, I. Effect of furfural concentration on ethanol production using Saccharomyces cerevisiae in an immobilized cells stirred-tank bioreactor with glucose-based medium and mathematical modeling. *J. Food Process. Preserv.* **2021**, *45*, e14635. [CrossRef]

Disclaimer/Publisher's Note: The statements, opinions and data contained in all publications are solely those of the individual author(s) and contributor(s) and not of MDPI and/or the editor(s). MDPI and/or the editor(s) disclaim responsibility for any injury to people or property resulting from any ideas, methods, instructions or products referred to in the content.